Comparison of 2D-and 3D-culture models as drug-testing platforms in breast cancer

Imamura, Yoshinori ; Mukohara, Toru ; Shimono, Yohei ; Funakoshi, Yohei ; Chayahara, Naoko ; Toyoda, Masanori ; Kiyota, Naomi ; Takao, Shintar…

(URL)
https://hdl.handle.net/20.500.14094/90003408

Comparison of 2D- and 3D-culture models as drug-testing platforms in breast cancer

YOSHINORI IMAMURA[1], TORU MUKOHARA[1,4], YOHEI SHIMONO[1,2], YOHEI FUNAKOSHI[1],
NAOKO CHAYAHARA[1], MASANORI TOYODA[1], NAOMI KIYOTA[1], SHINTARO TAKAO[3],
SEISHI KONO[3], TETSUYA NAKATSURA[5] and HIRONOBU MINAMI[1,4]

[1]Division of Medical Oncology/Hematology, Department of Medicine, [2]Division of Molecular and Cellular Biology,
Department of Biochemistry and Molecular Biology, and [3]Division of Breast and Endocrine Surgery, Department of Surgery,
Kobe University Graduate School of Medicine; [4]Cancer Center, Kobe University Hospital, Kobe, Hyogo; [5]Division of Cancer
Immunotherapy, Exploratory Oncology Research and Clinical Trial Center, National Cancer Center, Kashiwa, Chiba, Japan

Abstract. It is becoming recognized that screening of oncology drugs on a platform using two-dimensionally (2D)-cultured cell lines is unable to precisely select clinically active drugs; therefore three-dimensional (3D)-culture systems are emerging and show potential for better simulating the *in vivo* tumor microenvironment. The purpose of this study was to reveal the differential effects of chemotherapeutic drugs between 2D- and 3D-cultures and to explore their underlying mechanisms. We evaluated differences between 2D- and 3D-cultured breast cancer cell lines by assessing drug sensitivity, oxygen status and expression of Ki-67 and caspases. Three cell lines (BT-549, BT-474 and T-47D) developed dense multicellular spheroids (MCSs) in 3D-culture, and showed greater resistance to paclitaxel and doxorubicin compared to the 2D-cultured cells. An additional three cell lines (MCF-7, HCC-1954, and MDA-MB-231) developed only loose MCSs in 3D, and showed drug sensitivities similar to those found in the 2D-culture. Treatment with paclitaxel resulted in greater increases in cleaved-PARP expression in the 2D-culture compared with the 3D-culture, but only in cell lines forming dense 3D-MCSs, suggesting that MCS formation protected the cells from paclitaxel-induced apoptosis. Hypoxia was observed only in the dense 3D-MCSs. BT-549 had fewer cells positive for Ki-67 in 3D- than in 2D-culture, suggesting that the greater G0-dormant subpopulation was responsible for its drug resistance in the 3D-culture. BT-474 had a lower level of caspase-3 in the 3D- than in the 2D-culture, suggesting that the 3D-environment was anti-apoptotic. Finally, we compared staining for Ki-67 and caspases in the 2D- and 3D-primary-cultured cells originating from a patient-derived xenograft (PDX), fresh PDX tumor, and the patient's original tumor; 2D-cultured cells showed greater proportions of Ki-67-positive and caspase-3-positive cells, in agreement with the view that 3D-primary culture better represents characteristics of tumors *in vivo*. In conclusion, 3D-cultured cells forming dense MCSs may be better than 2D-cultured cells in simulating important tumor characteristics *in vivo*, namely hypoxia, dormancy, anti-apoptotic features and their resulting drug resistance.

Introduction

The number of patients suffering from cancers worldwide is increasing, and one of the most challenging issues in oncology continues to be the problem of developing active drugs economically and in a timely manner. In fact, the likelihood of approval from pre-clinical discovery to phase I clinical trial is lowest for oncology drugs (7%) compared with drugs for other indications (1). Considering the high cost and time-consuming nature of the clinical development of oncology drugs, better pre-clinical platforms for drug screening are urgently required.

Traditionally, the activity of anticancer drugs has been evaluated in two-dimensionally (2D)-cultured cancer cell lines. However, it is now being recognized that 2D-cultured cells are unable to simulate the microenvironment of the original tumors, which grow three-dimensionally (3D) (2-7). This is speculated to be relevant to the fact that many drugs proving to be clinically futile were pre-clinically evaluated to be 'active' using 2D-cultured cell line-based models. 3D-culture systems have received attention as a means to avoid certain drawbacks of 2D-culture models, by recapitulating the tumor microenvironment, at least in part (2-7).

In the present study, to investigate the utility of 3D-culture models in testing the activity of chemotherapeutic drugs, we compared 2D- and 3D-culture of breast cancer cell lines and primary cells obtained from a breast cancer patient and grown as a patient-derived xenograft (PDX).

Correspondence to: Dr Toru Mukohara, Cancer Center, Kobe University Hospital, 7-5-2 Kusunoki-cho, Chuo-ku, Kobe, Hyogo 650-0017, Japan
E-mail: mukohara@med.kobe-u.ac.jp

Table I. Drug concentrations applied.

| | Package insert data | | | | | | |
Drug name	Dose (mg/m^2)	Maximum drug concentration (μg/ml)	AUC (μg·h/ml)	MW	Clinical dose for breast cancer (mg/m^2)	Estimated AUC (μM·h)	Concentration for cell exposure (1x of AUC, μM)
PTX	180	4.47±1.29	16.46±3.76	853.91	175	13.66	0.19
ADR	50	8.70±2.73	62.40±40.7	579.98	60	43.35	0.60
5FU	-	-	20-24	130.08	-	2.86	0.04

The pharmacokinetic parameters of PTX and ADR are based on the Japanese package insert data. For 5FU, the optimal area under the curve (AUC) quoted in a previous study was employed. The final concentrations for cell exposure are calculated in accordance with the AUC, molecular weight (MW), clinical dose indicated for breast cancer (for PTX and ADR), and exposure time (72 h). PTX, paclitaxel; ADR, doxorubicin; 5FU, 5-fluorouracil.

Materials and methods

Breast cancer cell lines and PDX. Two estrogen receptor (ER)-positive/*HER2*-non-amplified (luminal-type; T-47D and MCF-7), two ER-negative/*HER2*-amplified (HER2-type; BT-474 and HCC-1954) (8), and two ER-negative/*HER2*-non-amplified (triple-negative type; BT-549 and MDA-MB-231) (8) breast cancer cell lines were purchased from the American Type Culture Collection (ATCC, Manassas, VA, USA). The cells were maintained in RPMI-1640® (Sigma-Aldrich, St. Louis, MO, USA) supplemented with 10% fetal bovine serum (FBS; Gemini-Bio-Products, Inc., Woodland, CA, USA), 100 U/ml penicillin, 100 U/ml streptomycin, and 2 mM glutamine. All cells were cultured at 37°C in a humidified atmosphere with 5% CO_2 and were in logarithmic growth phase upon initiation of the experiments. The cells were passaged for ≤3 months before fresh cells were obtained from frozen early passage stocks received from the supplier.

The breast cancer tissue sample was collected from a surgically resected primary tumor from a patient who underwent surgery at Kobe University Hospital. The patient gave informed consent for the research use of the tumor samples, as approved by the Research Ethics Board at Kobe University Graduate School of Medicine. The generation of PDX was as previously described (9). In brief, the breast cancer tissues were cut into fragments (~1 mm^3 in size) using a razor blade, and 4x10^6 cells were transplanted orthotopically into inguinal mammary fat pad regions of female NOD-SCID mice (Clea, Tokyo, Japan). When the size of the tumors reached ~1-2 cm in diameter, the mice were sacrificed, and the xenograft tumor was excised. In this study, a piece of fresh PDX tissue originating from a luminal-type breast cancer tumor was disaggregated by automated mechanical method (Medimachine®; Azone, Osaka, Japan). The primary cells were cultured in Dulbecco's modified Eagle's medium/nutrient mixture F12® (Life Technologies, Grand Island, NY, USA) supplemented with 2% FBS, 100 U/ml penicillin and 100 U/ml streptomycin, and cultured at 37°C in a humidified atmosphere with 5% CO_2. All animal experiments were carried out under the approval of the Kobe University Medical School Animal Care and Use Committee.

Drugs. Paclitaxel (PTX), doxorubicin (ADR), and 5-fluorouracil (5FU) were purchased from Wako (Osaka, Japan). Stock solutions were prepared in dimethyl sulfoxide (DMSO) and stored at 20°C. The drugs were diluted in fresh media before each experiment, with final DMSO concentrations <0.1%.

Drug sensitivity test. Cells (100 μl/well, n=6) were plated (day 0) in 2D plates [Falcon 96-well Tissue Culture Plate® (353072); Corning Inc., NY, USA] or 3D plates [NanoCluture 96-well Plate® (NCP-LH-96); SCIVAX, Kanagawa, Japan]. The numbers of cells seeded per well were as follows (determined in a preparatory experiment): BT-474, 5,000 (2D) and 15,000 cells/well (3D); T-47D, MCF-7 and BT-549, 2,500 (2D) and 10,000 cells/well (3D); HCC-1954, 1,000 (2D) and 5,000 cells/well (3D); MDA-MB-231, 500 (2D) and 2,500 cells/well (3D). Drugs were added on day 3. The concentration of each drug was adjusted to achieve 0.1, 1 and 10x the areas under the curve (AUC) obtained in clinical pharmacokinetic studies (Table I) (10). The number of viable cells was evaluated using a CellTiter-Glo® luminescent assay (Promega, Madison, WI, USA) on day 6. A series of bright field images were recorded on days 0-6 using a BZ-X710® inverted microscope (Keyence, Osaka, Japan).

Protein extraction and western blotting. Cells treated with PTX (1x the AUC, Table I) were washed once with ice-cold PBS and scraped immediately after adding lysis buffer [20 mM Tris (pH 7.5), 150 mM NaCl, 2 mM EDTA, 10% glycerol, 1% NP40] containing protease and phosphatase inhibitors (100 mM NaF, 1 mM phenylmethylsulfonyl fluoride, 1 mM Na_3VO_4, 2 mg/ml aprotinin, 5 mg/ml leupeptin). Cell lysates were centrifuged at 14,000 x g for 10 min at 4°C to pellet insoluble material, and the supernatant protein extracts were collected. Aliquots of protein extracts were separated by electrophoresis on precast 7.5% polyacrylamide gels, followed by transfer to polyvinylidene difluoride membranes. Membranes were probed with an antibody to detect cleaved poly(ADP-ribose) polymerase (PARP) (Asp214)(D64E10) (1:1,000; #5625; Cell Signaling Technology Beverly, MA, USA), and separately with a β-actin antibody (1:3,000; A1978; Sigma-Aldrich). Each primary antibody was detected using
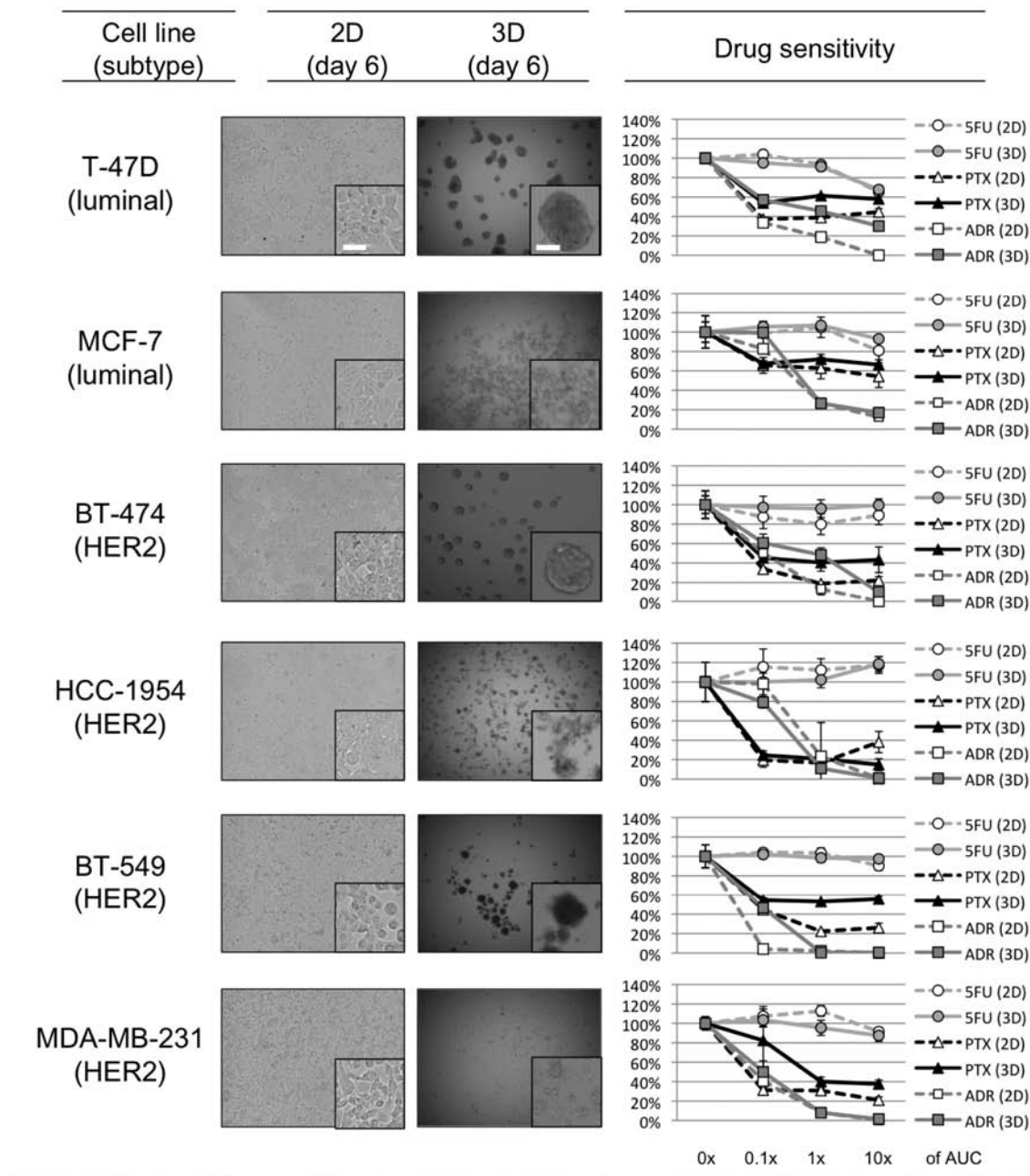
Figure 1. Effect of chemotherapeutic drugs on the cell growth of 2D- and 3D-cultured breast cancer cell lines. Six breast cancer cell lines were seeded on day 0 and cultured in 2D- or 3D-conditions through day 6 (left column). Brightfield images of each cell line were captured on day 6 (right column). Each cell line was treated with or without PTX, ADR or 5FU from day 3 through day 6. The number of viable cells present on day 6 is shown relative to that of the control cells without drug. Dashed lines represent 2D-culture and solid lines represent 3D-culture. Each data point represents the mean value and standard deviation of 6 replicate wells. Scale bars indicate 100 μm.

Amersham ECL Plus Western Blotting Detection Reagents (GE Healthcare, Buckinghamshire, UK).

Hypoxia assay. Cells in maintenance media were plated (day 0) in 2D (Corning Inc.) or 3D 96-well plates (SCIVAX), as described above. The hypoxia probe LOX-1® (SCIVAX) was added on day 3. LOX-1 is a phosphorescent light-emitting iridium complex; its phosphorescence, which is quenched by oxygen, and increases in response to low levels of oxygen, can be monitored using a fluorescence microscope (11). A BZ-X710 microscope was used to record the fluorescence images on day 4.

Histologic and immunohistochemical examinations. Cells were harvested by scraping into 7.5% formalin. On the following day, the sediment containing the cell button was scooped out and processed into paraffin wax. The paraffin-embedded cell button (cell block) was sectioned at a 4-μm thickness and these were assessed immunohistochemically using the following primary antibodies: Ki-67 (1:5; #IR626; Dako, Glostrup, Denmark), caspase-3 (1:200; #NCL-CPP32; Leica-Novocastra, Newcastle upon Tyne, UK), and caspase-8 (1:150; #NCL-CASP-8; Leica-Novocastra). For antigen retrieval, a citrate buffer (pH 6.0) was used for 10 min at 100°C and 30 min cooling to room temperature. A MACH 2 Double
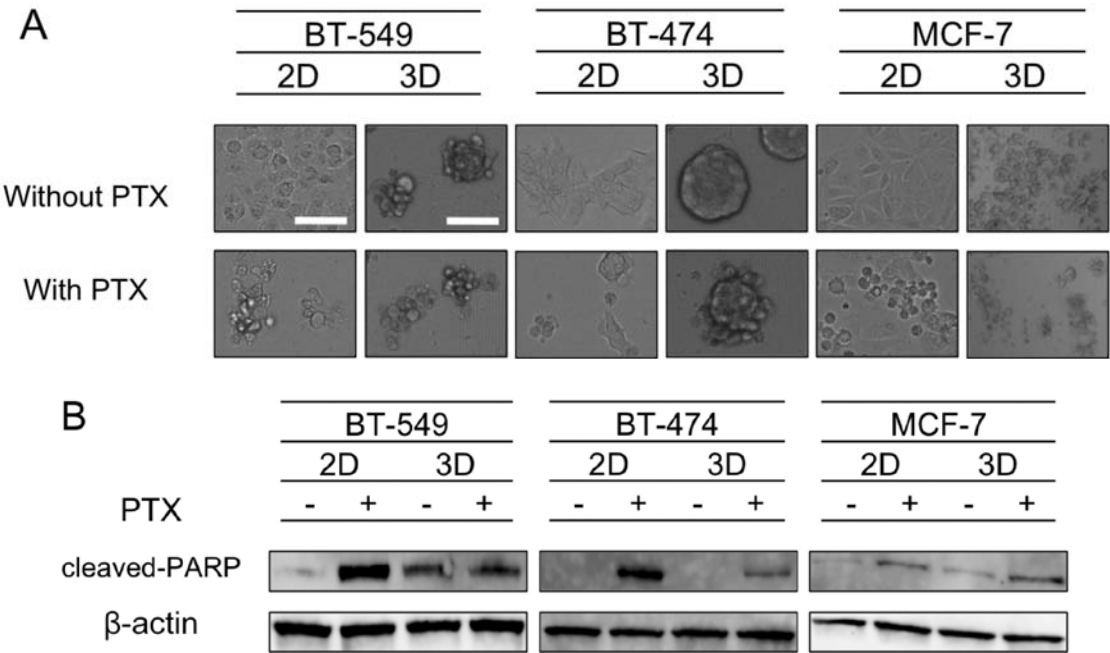
Figure 2. Effect of PTX on the apoptosis in 2D- and 3D-cultured breast cancer cell lines. (A) Brightfield images of each cell line grown with or without PTX (1x AUC) for three days. Scale bars indicate 100 μm. (B) Lysates of breast cancer cells propagated in 2D- and 3D-cultures were immunoblotted to detect cleaved PARP, which indicates cell apoptosis. Blots were stripped and re-probed for β-actin as a loading control.

Stain system (Biocare Medical, Concord, CA, USA) was used to detect antigen-antibody reactions, followed by brown coloring by DAB staining. Appropriate positive controls were employed for all conditions.

Results

Spheroid formation in 3D-culture. Approximately one day after seeding on 3D-culture plates, 3 of the 6 breast cancer cell lines, T47-D, BT-474 and BT-549, started to form dense multicellular spheroids (MCSs). The size of these MCSs plateaued ~3 days after seeding, and the maximal size of the spheroids was ~200-300 μm for each of these cell lines. For MCF-7, HCC-1954 and MDA-MB-231, the cells accumulated in the 3D-culture plates somewhat more than in the 2D-culture plates, and although spheroids formed, they were looser than those produced by the other 3 cell lines (Fig. 1).

Drug sensitivity in 2D- and 3D-culture. The relative growth rate of the 6 breast cancer cell lines in the presence or absence of the 3 chemotherapeutic agents (PTX, ADR, and 5FU) in 2D- or 3D-cell culture is shown in Fig. 1. The range of drug concentrations used was set based on clinical pharmacokinetic data (0.1, 1, and 10x the AUC; Table I) in order to explore the clinical relevance of the results. For 5FU, there was no clear difference in sensitivity between the 2D- and 3D-culture in any of the cell lines tested. The 3 cell lines that developed dense 3D-MCSs (T-47D, BT-474 and BT-549) tended to show relative resistance to PTX and ADR in the 3D-culture as compared to this resistance in 2D. In contrast, the other 3 that developed loose 3D-spheroids (MCF-7, HCC-1954 and MDA-MB-231) tended to have similar sensitivity to PTX and ADR in the 2D- and 3D-culture. These findings confirm that the formation of dense MCSs in

3D-culture plays a role in determining the sensitivity of the cell lines to PTX and ADR.

Apoptosis induced by PTX. To explore the mechanism of differential sensitivity to PTX in the 2D- and 3D-cultures, 3 cell lines were subjected to further study; BT-549 and BT-474 as representatives of cell lines forming dense 3D-MCSs, and MCF-7 as an example of the loose 3D phenotype. Fig. 2A shows that for BT-549 and BT-474 cells, exposure to PTX (1x the AUC) resulted in cell shrinkage, indicative of apoptosis when grown in 2D-culture, yet dense 3D-MCSs remained in the 3D-cultures. The same PTX treatment of MCF-7 cells yielded significant cell shrinkage in both the 2D- and 3D-cultures (Fig. 2A). Consistent with these findings, treatment of BT-549 or BT-474 cells with PTX resulted in much smaller increases in cleaved PARP in the 3D-culture than in the 2D-culture, whereas in MCF-7 (with loose MCSs) the same PTX treatment resulted in a similar degree of increase in cleaved PARP (Fig. 2B). These results confirmed that relative resistance to PTX in the cell lines with dense MCSs in 3D-culture than in 2D-culture was in part due to reduced apoptosis.

Hypoxia in dense MCSs. It has been speculated that the formation of dense MCSs leads to hypoxia inside the spheroids mimicking *in vivo* tumors, and hypoxia is known to be one of the factors associated with resistance to chemotherapeutic drugs (12). Therefore, we evaluated the oxygen status in 2D- and 3D-cultures by utilizing the hypoxia probe LOX-1, that generates signals that are visible using a fluorescence microscopy. As shown in Fig. 3, hypoxic areas were observed inside the dense 3D-MCSs from the BT-549 and BT-474 cell lines, but not in the loose spheroids formed by MCF-7 cells or cells grown in 2D. These findings suggest that the hypoxia status in dense 3D-MCSs may be one of the causes of their drug resistance.
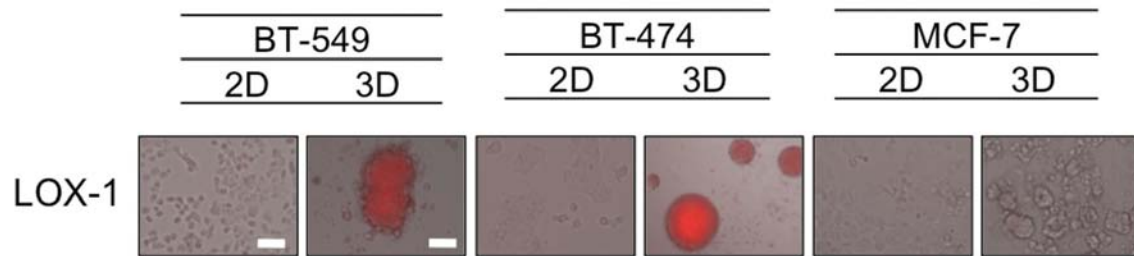
Figure 3. Hypoxic status in 3D-MCSs. Each cell line was allowed to grow in a 2D- or 3D-culture for three days and then the hypoxia probe LOX-1 was applied for 24 h and cells were imaged by a fluorescence microscopy to reveal oxygen levels. Scale bars indicate 100 μm.
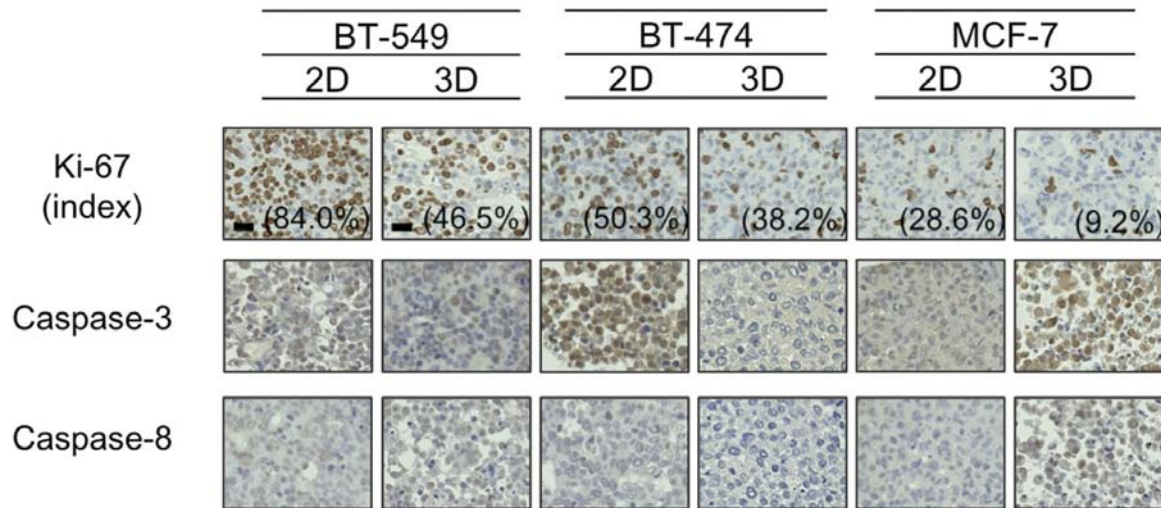

Figure 4. Expression of Ki-67 and caspases in 2D- and 3D-cultured breast cancer cell lines. Representative brightfield images are shown for the immunohisto-chemical staining (brown) for Ki-67, caspase-3, and caspase-8 in 2D- and 3D-cultured breast cancer cell lines. Scale bars indicate 100 μm.

Ki-67 and caspase expression. Hypoxia has been reported to cause cancer cell dormancy in the G0 phase (13), thus we next evaluated staining using the antibody Ki-67, which is reported to be positive in cells except for those in the G0 phase. As shown in Fig. 4, the Ki-67 index was higher in the 2D-culture than that in the 3D-culture for all 3 cell lines tested. The difference was particularly marked for the BT-549 cells, which formed dense 3D-MCSs (84.0% Ki-67-positive cells in 2D vs. 46.5% in 3D).

Following this, due to a study suggesting that downregulation of caspase-3 and -8 in hypoxic conditions may mediate resistance to PTX in breast cancer cells (14), we immuno-histochemically evaluated the expression of these proteins in 2D- and 3D-cultures. As shown in Fig. 4, the expression levels of caspase-3 and -8 were almost identical between the 2D- and 3D-cultures for all 3 cell lines tested, with the exception of BT-474 cells, in which caspase-3 expression was much higher in the 2D-culture than this level in the 3D-culture. In addition, caspase-3 was detected mainly in the nuclei of 2D-cultured BT-474 cells, indicative of active caspase-3. These findings suggested to us that hypoxia in 3D-MCSs may lead to cell dormancy and/or downregulation of caspase-3, and result in resistance to PTX.

The potential of the 3D-primary culture to simulate tumor growth in vivo. To explore the relevance of a 3D-culture to

tumor growth *in vivo*, we compared an excised tumor and its 2D- and 3D-primary cultures in terms of expression of Ki-67, caspase-3, and caspase-8. We utilized a PDX tumor for this purpose. As shown in Fig. 5, the proportion of cells positive for Ki-67 in the 2D- and 3D-primary cultured cells originating from PDX, fresh PDX tumor, and the patient's original tumor were 77.4, 57.4, 41.6 and 34.1%, respectively. Moreover, consistent with the BT-474 cells (Fig. 4), caspase-3 expression was much higher in the PDX tumor and its 2D-primary culture than in its 3D-primary culture, whereas no difference was observed in caspase-8 expression between the 2D- and 3D-culture. These findings confirm that a 3D-primary culture rather than a 2D-primary culture may better indicate *in vivo* tumor dormancy and anti-apoptotic features.

Discussion

In the present study, we demonstrated that certain breast cancer cell lines formed dense 3D-MCSs, and the formation of MCSs was associated with decreased sensitivity to chemotherapeutic drugs (Fig. 1). Our data also revealed that the drug resistance may be caused by hypoxia in MCSs, which was associated with an increased cell population in the G0 phase and/or downregulation of pro-apoptotic molecules such as caspase-3 (Figs. 2-4). Moreover, tumor dormancy observed in the *in vivo*
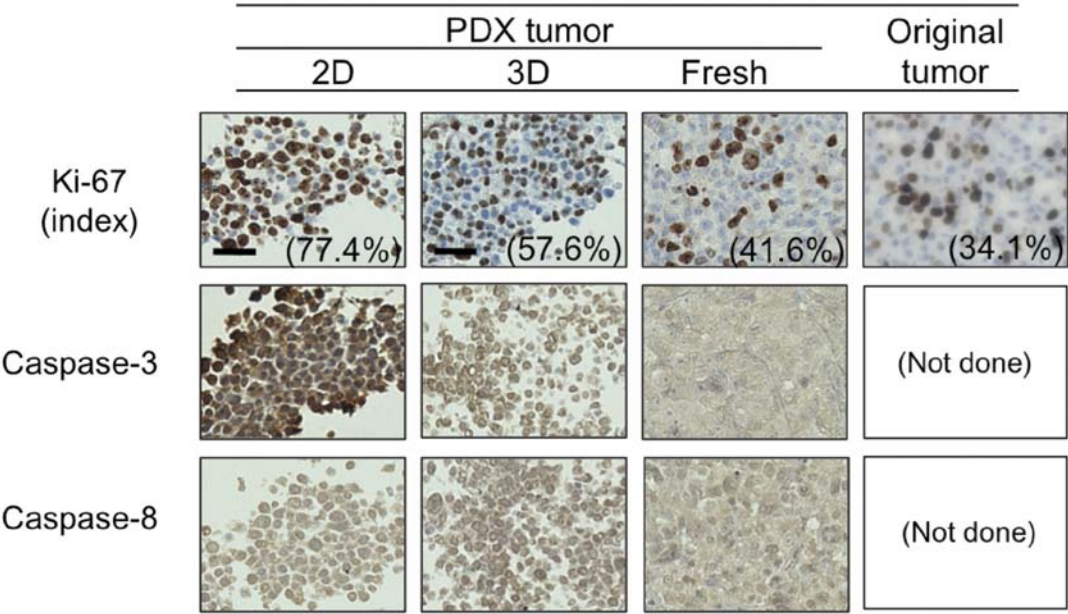
Figure 5. Expression of Ki-67 and caspases in a PDX and its 2D- and 3D-primary-cultured cells. Representative brightfield images are shown for the immunohistochemical staining (brown) for Ki-67, caspase-3, and caspase-8 in 2D- and 3D primary-cultured cells originating from PDX, fresh PDX tumor, and the patient's original tumor (Ki-67 only). Scale bars indicate 100 μm.

PDX tumor was better represented by its 3D-primary culture than its 2D-primary culture (Fig. 5).

2D-cultured cancer cell lines grown on plastic surfaces are considered unable to precisely simulate tumor conditions *in vivo* (2-7). It may therefore, be predicted that the development of anticancer drugs based on screening using 2D-cultured cell lines is not efficient. The fact that numerous anticancer drugs are eliminated during clinical development indicates that anticancer activity tends to be overestimated on a 2D-culture-based screening platform. In contrast, 3D-culture systems have been shown to better simulate the *in vivo* tumor microenvironment than a 2D-culture (3-7); several previous studies have shown that 2D-cultured cells tended to overestimate the efficacies of chemotherapeutic drugs compared with 3D-cultured cells (15-17). Consistent with these studies, our present study showed that the cell lines producing dense 3D-MCSs are more resistant to PTX and ADR in a 3D- than in 2D-culture (Fig. 2A). When measuring PTX-induced apoptosis, this tendency was even more apparent (Fig. 2B), suggesting that the formation of 3D-MCSs may protect cells from cell death. These findings suggest that a 3D-culture potentially avoids the overestimation of antitumor efficacy observed in a 2D-culture. It is noteworthy that the phenomena were observed with the clinically achievable drug concentrations calculated based on the AUC in cancer patients, which were less than the maximum drug concentrations (Cmax, Table I). While drug concentrations around Cmax have conventionally been employed for testing in *in vitro* experiments, these concentrations may be inappropriate since Cmax does not persist for hours *in vivo* (18). Therefore, we believe that drugs which kill 3D-growing cells at concentrations less than Cmax should be evaluated to be active.

Potential advantages of 3D-culture systems over 2D-culture systems are that only the former may feature oxygen gradients which exist in *in vivo* tumors. Hypoxia is known to cause drug resistance through several mechanisms. One conventional mechanism is that of hypoxia-induced cell cycle arrest. Sullivan *et al* demonstrated that hypoxia induced an increased G0 non-cycling population associated with etoposide resistance in breast cancer cell lines (13). Consistent with this result, one of the cell lines forming dense MCSs in 3D, BT-549, had a much lower Ki-67 labeling index (representing a greater G0 population) in the 3D than that in the 2D-cultured cells. However, another cell line that formed dense 3D-MCSs, BT-474, had only a slightly lower Ki-67 in 3D than in 2D, with a difference of 12.1% (Fig. 4), which was actually smaller than that in MCF-7 cells which formed only loose MCSs. This indicated that drug resistance associated with dense 3D-MCSs could not always be attributable to an increased G0-dormant cell population. Therefore, we evaluated the expression of caspase-3 and -8, as the downregulation of these two pro-apoptotic molecules, along with change in expression of another six molecules, were identified to be potentially involved in hypoxia-induced protection against PTX-induced apoptosis by a previous study (14). Partially consistent with this study, BT-474 expressed lower levels of caspase-3 in the 3D- than in 2D-culture. Furthermore, we found that tumor dormancy and downregulation of caspase-3 observed in the original patient tumor and/or PDX tumor was better maintained in the 3D-primary cultured cells than in the 2D-primary cultured cells (Fig. 5). These findings suggest that 3D-culture may provide a better drug screening platform; one that produces more clinically relevant results.

Several limitations of our study warrant mention. Firstly, this study was derived from the nature of an *in vitro* model. At present, there are various 3D-culture systems besides the one we used, yet none of them are considered to be a standard method, and it is unclear which system is the most clinically relevant (3-7). One clear observation is that 3D-culture of cell lines will never accurately, fully represent the tumor

microenvironment *in vivo*, because the latter have interactions with stromal tissues or blood perfusions. Co-culture with stromal cells or primary culture in 3D-conditions may partially solve these issues and are under investigation in our laboratory. Animal models such as PDXs are being evaluated as a potential drug screening platform for the next generation (19-22), however, difficulty in the development and expansion of the PDX model, and their high-cost will preclude their use in high-throughput screening. Therefore, refining 3D-culture systems as drug screening platforms is worth driving forward. Secondly, although our results support that hypoxia in 3D-culture may play a role in drug resistance, we did not prove the underlying molecular mechanisms of this in the present study. In addition, we did not explore many other potential mechanisms of drug resistance induced by hypoxia, such as enhanced drug efflux or autophagy, or inhibition of senescence or DNA damage (12,23). These mechanisms of hypoxia-induced drug resistance are reported to be mediated mainly by hypoxia-inducible factor-1α (HIF-1α) (12,24,25). In our study, however, we were unable to detect HIF-1α with immunohistochemistry or western blotting, even in dense MCSs (data not shown).

In conclusion, 3D-cultured breast cancer cells show relative drug resistance as compared to 2D-cultured cells when forming dense 3D-MCSs, and the resistance is associated with hypoxia. 3D-MCSs could be utilized as an *in vitro* cell-based drug-testing platform.

Acknowledgements

References

1. Hay M, Thomas DW, Rosenthal J, *et al*: Clinical development success rates for investigational drugs. Nat Biotechnol 32: 40-51, 2014.
2. Yamada KM and Cukierman E: Modeling tissue morphogenesis and cancer in 3D. Cell 130: 601-610, 2007.
3. Hirschhaeuser F, Menne H, Kunz-Schughart LA, *et al*: Multicellular tumor spheroids: an underestimated tool is catching up again. J Biotechnol 148: 3-15, 2010.
4. Rimann M and Graf-Hausner U: Synthetic 3D multicellular systems for drug development. Curr Opin Biotechnol 23: 803-809, 2012.
5. Breslin S and O'Driscoll L: Three-dimensional cell culture: the missing link in drug discovery. Drug Discov Today 18: 240-249, 2013.
6. Lovitt CJ, Shelper TB and Avery VM: Advanced cell culture techniques for cancer drug discovery. Biology 3: 345-367, 2014.
7. Weigelt B, Ghajar CM and Bissell MJ: The need for complex 3D culture models to unravel novel pathways and identify accurate biomarkers in breast cancer. Adv Drug Deliv Rev 69-70: 42-51, 2014.
8. Lacroix M and Leclercq G: Relevance of breast cancer cell lines as models for breast tumours: an update. Breast Cancer Res Treat 83: 249-289, 2004.
9. Nobutani K, Shimono Y, Takai Y, *et al*: Absence of primary cilia in cell cycle-arrested human breast cancer cells. Genes Cells 19: 141-152, 2014.
10. Gamelin E, Delva R, Jacob J, *et al*: Individual fluorouracil dose adjustment based on pharmacokinetic follow-up compared with conventional dosage: results of a multicenter randomized trial of patients with metastatic colorectal cancer. J Clin Oncol 26: 2099-2105, 2008.
11. Zhang S, Hosaka M, Yoshihara T, *et al*: Phosphorescent light-emitting iridium complexes serve as a hypoxia-sensing probe for tumor imaging in living animals. Cancer Res 70: 4490-4498, 2010.
12. Rohwer N and Cramer T: Hypoxia-mediated drug resistance: novel insights on the functional interaction of HIFs and cell death pathways. Drug Resist Updat 14: 191-201, 2011.
13. Sullivan R and Graham CH: Hypoxia prevents etoposide-induced DNA damage in cancer cells through a mechanism involving hypoxia-inducible factor 1. Mol Cancer Ther 8: 1702-1713, 2009.
14. Flamant L, Notte A, Michiels C, *et al*: Anti-apoptotic role of HIF-1 and AP-1 in paclitaxel exposed breast cancer cells under hypoxia. Mol Cancer 9: 191, 2010.
15. Karlsson H, Fryknas M, Nygren P, *et al*: Loss of cancer drug activity in colon cancer HCT-116 cells during spheroid formation in a new 3-D spheroid cell culture system. Exp Cell Res 318: 1577-1585, 2012.
16. Vinci M, Gowan S, Boxall F, *et al*: Advances in establishment and analysis of three-dimensional tumor spheroid-based functional assays for target validation and drug evaluation. BMC Biol 10: 29, 2012.
17. Lee JM, Mhawech-Fauceglia P, Lee N, *et al*: A three-dimensional microenvironment alters protein expression and chemosensitivity of epithelial ovarian cancer cells in vitro. Lab Invest 93: 528-542, 2013.
18. No authors listed: Dishing out cancer treatment. Nat Biotechnol 31: 85, 2013.
19. Marangoni E, Vincent-Salomon A, Auger N, *et al*: A new model of patient tumor-derived breast cancer xenografts for preclinical assays. Clin Cancer Res 13: 3989-3998, 2007.
20. Cottu P, Marangoni E, Assayag F, *et al*: Modeling of response to endocrine therapy in a panel of human luminal breast cancer xenografts. Breast Cancer Res Treat 133: 595-606, 2012.
21. Zhang X, Claerhout S, Prat A, *et al*: A renewable tissue resource of phenotypically stable, biologically and ethnically diverse, patient-derived human breast cancer xenograft models. Cancer Res 73: 4885-4897, 2013.
22. Fong EL, Martinez M, Yang J, *et al*: Hydrogel-based 3D model of patient-derived prostate xenograft tumors suitable for drug screening. Mol Pharm 11: 2040-2050, 2014.
23. Housman G, Byler S, Sarkar S, *et al*: Drug resistance in cancer: an overview. Cancers 6: 1769-1792, 2014.
24. Li J, Shi M, Cao Y, *et al*: Knockdown of hypoxia-inducible factor-1alpha in breast carcinoma MCF-7 cells results in reduced tumor growth and increased sensitivity to methotrexate. Biochem Biophys Res Commun 342: 1341-1351, 2006.
25. Doublier S, Belisario DC, Sapino A, *et al*: HIF-1 activation induces doxorubicin resistance in MCF7 3-D spheroids via P-glycoprotein expression: a potential model of the chemo-resistance of invasive micropapillary carcinoma of the breast. BMC Cancer 12: 4-18, 2012.